

# Sequence of phase transitions in a model of interacting rods

Juliane U. Klamser,<sup>1</sup> Tridib Sadhu,<sup>2</sup> and Deepak Dhar<sup>3</sup>

<sup>1</sup>*Gulliver UMR CNRS 7083, ESPCI Paris, Université PSL, 75005 Paris, France.*

<sup>2</sup>*Department of Theoretical Physics, Tata Institute of Fundamental Research, Mumbai 400005, India.*

<sup>3</sup>*Department of Physics, Indian Institute of Science Research and Education, Pune 411008, India.*

In a system of interacting thin rigid rods of equal length  $2\ell$  on a two-dimensional grid of lattice spacing  $a$ , we show that there are multiple phase transitions as the coupling strength  $\kappa = \ell/a$  and the temperature are varied. There are essentially two classes of transitions. One corresponds to the Ising-type spontaneous symmetry breaking transition and the second belongs to less-studied phase transitions of geometrical origin. The latter class of transitions appear at fixed values of  $\kappa$  irrespective of the temperature, whereas the critical coupling for the spontaneous symmetry breaking transition depends on it. By varying the temperature, the phase boundaries may cross each other, leading to a rich phase behaviour with infinitely many phases. Our results are based on Monte Carlo simulations on the square lattice, and a fixed-point analysis of a functional flow equation on a Bethe lattice.

PACS numbers: 05.40.Jc, 02.50.Cw, 87.10.Mn

Lattice models with interacting degrees of freedom are extensively studied in statistical mechanics [1, 2]. They remain instructive textbook examples for emergent phases and phase transitions. Especially in two dimensions, the marginal competition between fluctuations and order can lead to interesting phase behaviour. Yet, there are still surprises lurking even with the simplest kind of two-dimensional models. In this *Letter* we present one such example where we find less-studied geometrical transitions coexisting alongside conventional disorder-order transitions. An interplay between different mechanisms of these transitions yields a rich phase diagram with an infinity of phases. These features are expected to be not specific to the model studied here.

Our model is similar to the lattice-gases of rigid orientable molecules that were extensively studied for organic solids [3, 4], hydrogen bonded solvents [5], water [6], and adsorbed monolayers [7]. In these models, anisotropic structure blocks (molecules) are pivoted at regular lattice sites, but they can rotate while being constrained by steric interaction with neighbours. This makes them different from well-known lattice-gases of movable molecules [8–11], particularly the hard-rod models for isotropic-nematic transitions without a positional order in liquid crystals [12–15]. A counterpart of liquid crystals is plastic crystal phases [16–19] of organic solids, where molecules are ordered in position but can show a varying degree of orientational disorder. Plastic crystals show a sequence of phase transitions from one crystalline phase to another, when the temperature is lowered or the pressure is increased [19–22]. Our simple model captures this basic phenomenology.

In the simplest example we discuss in this *Letter*, non-polar thin rigid rods of length  $2\ell$  are pinned at their midpoint at the lattice sites of an  $L \times L$  square grid of lattice unit  $a$  and with periodic boundaries. Rods are free to rotate in the plane as illustrated in Fig. 1a. The orienta-

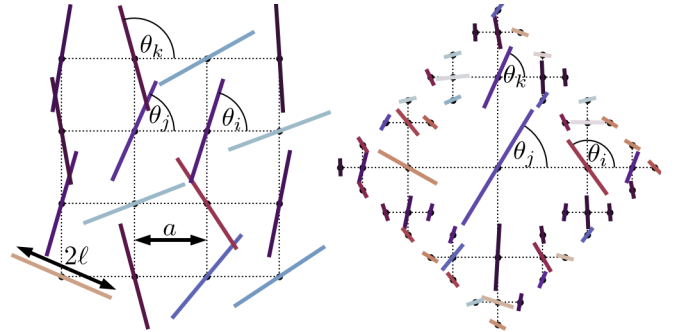


FIG. 1. (a) A configuration of rods on a square grid (dashed lines), where five overlaps between nearest-neighbour rods cost a total energy  $5U_1$ . (b) The model on a Bethe lattice (dashed lines), where, unlike the square lattice, only rods connected by a single lattice edge interact. All rods and lattice units have constant length,  $2\ell$  and  $a$  respectively. The varied scale in (b) is for representation purpose only.

tion of a rod at a site  $\mathbf{r}$  is specified by its angle  $\theta_{\mathbf{r}}$  with  $0 \leq \theta_{\mathbf{r}} < \pi$ . A configuration is given by the set of angles of all rods. Interactions between rods are solely due to overlaps, which costs a constant energy  $U_1$  for each nearest neighbour overlap,  $U_2$  for each next nearest neighbour overlap, and so on, no matter where they occur. The total energy of a configuration  $H = \sum_i n_i U_i$  with  $n_i$  being the number of  $i$ -th neighbour overlaps. Configurations are weighted by the canonical Boltzmann-Gibbs measure  $e^{-\beta H}$  where  $\beta$  is the inverse temperature. (Similar models of orientable anisotropic objects pivoted at lattice points have been studied in [23–25].)

Using Markov-Chain Monte Carlo (MCMC) simulations we show that the system undergoes infinitely many phase transitions as  $\beta$  and the coupling strength  $\kappa = \ell/a$  are varied. There are essentially two classes of transitions. One that belongs to the disorder-order transition, where there is a breaking of the discrete symmetry group

of the orientations in the model. With increasing  $\kappa$ , as more neighbours interact, more symmetry breaking transitions take place, successively increasing the degree of orientational order. The second class of transitions induce singularities in the angular distribution of rods  $P(\theta)$ . These transitions are related to singular changes in the geometry of overlap manifold and we refer to them as geometrical transitions. They are induced by non-analyticities in the interaction potential between the rods as a function of the distance between them, which, unlike the disorder-order transition, do not depend on  $\beta$ . Each geometrical and symmetry-breaking transition may be characterized by a different order parameter and an interplay between these transitions leads to infinitely many phases on the  $(\beta, \kappa)$  plane.

The model is generalizable to arbitrary lattices and higher dimensions. In particular, we discuss the model on a Bethe lattice shown in Fig. 1b, where the distribution of angular orientation is obtained from a fixed point solution of a functional equation corresponding to the self-consistency condition on the Bethe lattice.

*Probability distribution of orientations* — For the model on a square lattice, first few transitions for small  $\kappa$  are shown in the distribution  $P(\theta)$  in Fig. 2 for soft repulsive rods at  $\beta = 1.4$ , with  $U_i = 1$  for all  $i$ . For  $\kappa < 1/2$ , rods do not interact and  $P(\theta)$  is uniform. For larger  $\kappa$ , the distribution develops a non-trivial profile with  $P(\theta)$  constant in some range, and not in others, but has the four-fold symmetry of the lattice (see Fig. 2a). The extent of the regions with constant  $P(\theta)$  decreases with increasing  $\kappa$  and vanishes for  $\kappa \simeq 0.707$ . As  $\kappa$  crosses this value, the local maximum of  $P(\theta)$  along the diagonal directions  $\theta = \{\pi/4, 3\pi/4\}$  becomes a local minimum, and two pairs of cusp singularities emerge. The location of these cusp singularities move with  $\kappa$  and they are determined by the singularity in the overlap interaction. The next sharp change happens as  $\kappa$  crosses the value of one (see Fig. 2b). Firstly, two pairs of cusp singularities merge at  $\theta = \{0, \pi/2\}$  respectively. Secondly, the slope of  $P(\theta)$  near these angles changes sign, leading to a drop in  $P(\theta)$ . A third singular change in  $P(\theta)$  is at  $\kappa \simeq 1.252$  where the symmetry around  $\theta = \pi/2$  is spontaneously broken (see Fig. 2c). The probability  $P(\theta)$  is depleted in one of the sectors  $\theta \in (0, \pi/2)$  or  $\theta \in (\pi/2, \pi)$ , i.e. the majority of rods is preferentially aligned in either one of these sectors. In Fig. 2c, we show the case where the first angular sector is spontaneously selected. For  $\kappa \gtrsim 1.382$ , the reflection symmetry about  $\theta = \pi/4$  is spontaneously broken (see Fig. 2d).

The first and the second singular changes in  $P(\theta)$  (Fig. 2a and b) are about qualitative changes in the dependence of  $P(\theta)$  on  $\theta$  and correspond to the geometrical transitions. For example, in the range  $1/2 < \kappa < 1/\sqrt{2}$ ,  $P(\theta)$  has flat parts, in the range  $1/\sqrt{2} < \kappa < 1$ ,  $P(\theta)$  has two pairs of square-root-cusp singularities, and so on. The breakdown of symmetries of  $P(\theta)$  (Fig. 2c and d)

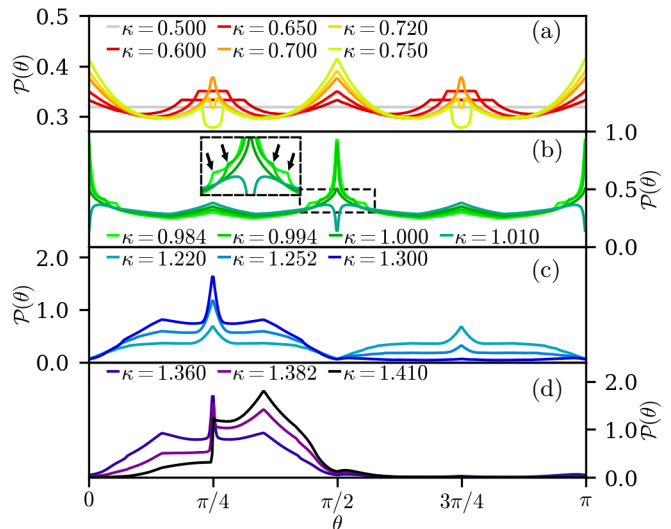


FIG. 2. Square lattice – (color online) Probability distribution of the orientation of rods at increasing values of  $\kappa$ . (a): As  $\kappa$  is increased from 0.5 to 0.75, two pairs of derivative discontinuities cross each other at  $\theta = \{\pi/4, 3\pi/4\}$  and become cusp singularities above  $\kappa \simeq 0.707$ . (b): The cusp singularities merge in pairs for  $\kappa = 1$  at  $\theta = \{0, \pi/2\}$ . Cusps are indicated by arrows in the zoom in the inset. (c): The symmetry around  $\theta = \pi/2$  still present for  $\kappa = 1.22$ , is broken for  $\kappa = 1.252$  and above. (d): In the angular range  $\theta \in (0, \pi/2)$  the symmetry around  $\pi/4$  present for  $\kappa = 1.360$  is lost for  $\kappa = 1.382$  and above. Results are for  $\beta = 1.4$  and  $U_i = 1$  for all  $i$  on an  $L \times L$  square lattice with  $L = 240$ .

correspond to disorder-order transitions. In the following we closely look at one from each class of transitions, namely, the geometrical transition at  $\kappa = 1$  and the spontaneous symmetry breaking transition at  $\kappa \simeq 1.252$ .

*Symmetry breaking at  $\kappa \simeq 1.252$*  — Considering the breakdown of  $P(\theta) = P(\pi - \theta)$  symmetry in Fig. 2c, it is expected that the transition belongs to the Ising class of disorder-order transitions. A measure of the long-range order set by the transition, is the norm  $|\Psi_2|$  of the bulk orientation vector  $\Psi_2 = \frac{1}{L^2} \sum_{\mathbf{r}} \exp(i2\theta_{\mathbf{r}})$ . (The observable is in analogy with the well-known nematic order parameter  $P_2(\cos\theta)$  in liquid crystals [26] and the bond-orientational order parameter  $\psi_6$  in the two-dimensional melting [27, 28].) The change in average  $|\Psi_2|$  is shown in Fig. 3a for various system sizes. Extrapolating the finite size effects to the thermodynamic limit gives  $|\Psi_2| = 0$  for  $\kappa$  below a critical value  $\kappa_c \simeq 1.252$  and  $|\Psi_2|$  non-zero above.

At an even higher value  $\kappa \simeq 1.382$ , above the onset of next-nearest-neighbour interactions,  $|\Psi_2|$  shows the signature of a second symmetry-breaking transition. Considering the broken symmetry in  $P(\theta)$  in Fig. 2d, we consider  $|\Psi_4| = |\frac{1}{L^2} \sum_{\mathbf{r}} \exp(i4\theta_{\mathbf{r}})|$  as an appropriate order parameter. Fig. 3b shows that while  $|\Psi_4|$  is insensitive to the first disorder-order transition, at the second transition it develops a singularity in the thermodynamic limit,

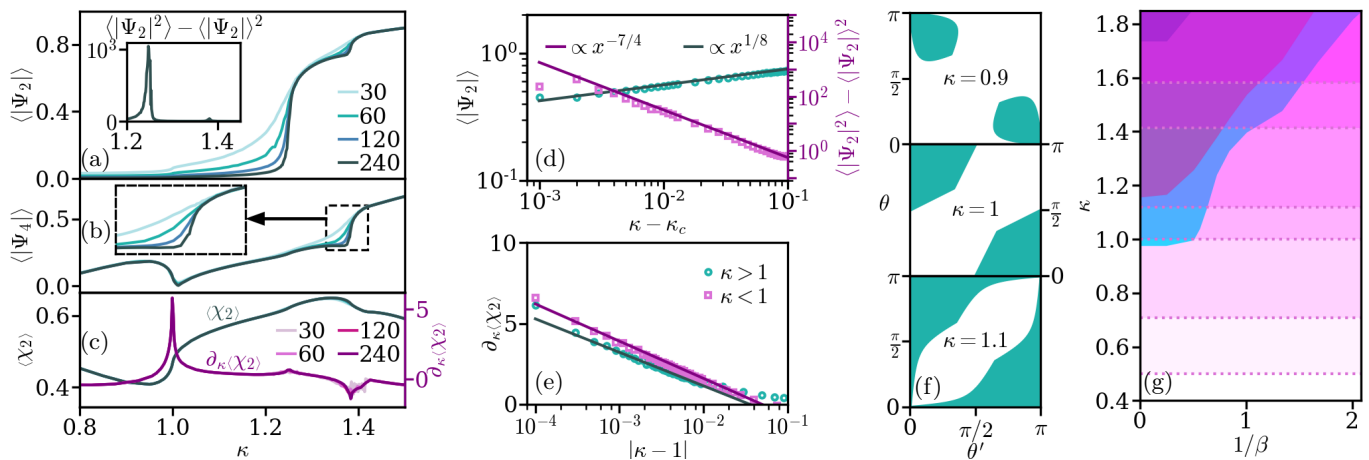


FIG. 3. Square lattice – (color online) (a): Mean amplitude of the bulk orientation vector  $|\Psi_2|$  for different system sizes  $L \times L$  (legend indicates linear system size  $L$ ) at  $\beta = 1.4$  showing around  $\kappa \simeq 1.252$  the typical finite-size behaviour of a continuous disorder-order transition. The variance of  $|\Psi_2|$ , shown in the inset for  $L = 240$ , exhibits a sharp peak at the transition. (b): Mean of order parameter  $|\Psi_4|$  for the second disorder-order transition at  $\kappa \simeq 1.382$ . A finite size dependence is shown in the inset. (c): Mean of bulk order parameter  $\chi_2$  shows an infinite slope at  $\kappa = 1$ , which reflects as divergence in  $\partial_\kappa \langle \chi_2 \rangle$ . Shown data is for the same  $\beta$  and system sizes as in (a), but curves are almost indiscernible from each other due to absence of finite size effects around  $\kappa = 1$ . (d): Power-law dependence of mean (round symbols) and variance (square symbols) of  $|\Psi_2|$  for  $\kappa \gtrsim \kappa_c$  for  $L = 240$  and  $\beta = 1.4$ . (e): Logarithmic divergence of  $\partial_\kappa \langle \chi_2 \rangle$  as  $\kappa$  approaches one from both sides for  $\beta = 1$  and  $L = 60$ . (f): Overlap region, filled with green color on the  $(\theta, \theta')$  plane, between  $x$ -nearest-neighbour rods of orientation  $\theta$  and  $\theta'$ . Boundary of the overlap region undergoes a sharp change as  $\kappa$  crosses one. (g): A sketch of the phase diagram where different coloured regions correspond to different phases. Dotted horizontal lines denote geometrical transitions. The remaining phase boundaries correspond to disorder-order transitions. They are estimated from peak positions of the variance of the appropriate bulk-orientation order parameter at discrete points in the phase space. Results are for  $U_i = 1$  for all neighbours  $i$ .

with a behavior at finite  $L$  consistent with the finite-size-scaling theory of continuous transitions. At increasing  $\kappa$ , there are more disorder-order transitions, induced by higher neighbour interactions, each breaking finer symmetries. While the function  $P(\theta)$  is expected to capture all these transitions, in a Ginzburg-Landau-Wilson theory description, one would need different order parameters for different transitions.

*Transition at  $\kappa = 1$*  – Considering the nature of changes in  $P(\theta)$  in Fig. 2b, we construct a bulk observable  $\chi_2 = \frac{1}{L^2} \sum_{\mathbf{r}} (\sin 2\theta_{\mathbf{r}})^2$  that shows a strong variation at  $\kappa = 1$  shown in Fig. 3c. We note two important features. First, there are no visible finite-size effects around  $\kappa = 1$  that could create an asymptotic singularity in the thermodynamic limit. Second, however, the slope of  $\chi_2$  becomes infinite at  $\kappa = 1$  even for small systems, hence leading to the divergence of  $\partial_\kappa \chi_2$ , although the orientational correlation length remains finite.

*Universality class* – The divergence in  $\partial_\kappa \chi_2$  at  $\kappa = 1$  is in contrast to the discontinuous change in  $\partial_\kappa |\Psi_2|$  at  $\kappa_c \simeq 1.252$ , consistent with the theoretical understanding of the different origins of the two transitions. This difference is further evident from the scaling of these singularities. For the disorder-order transition, the mean and the variance of  $|\Psi_2|$  follow a power-law with vanishing  $\kappa - \kappa_c$ ,

$$\langle |\Psi_2| \rangle \sim (\kappa - \kappa_c)^\beta; \quad \langle |\Psi_2|^2 \rangle - \langle |\Psi_2| \rangle^2 \sim (\kappa - \kappa_c)^{-\gamma}, \quad (1)$$

(see Fig. 3d) where the critical exponents  $\beta = 1/8$  and  $\gamma = 7/4$  are commensurate with the Ising exponents in two dimensions [1]. In comparison,  $\partial_\kappa \langle \chi_2 \rangle$  diverges logarithmically with  $|\kappa - 1|$  (see Fig. 3e).

*Geometric origin of logarithmic divergence* – The unusual logarithmic singularity at  $\kappa = 1$  has a subtle geometric origin. It relates to a non-analytic dependence of the overlap area in the  $(\theta, \theta')$ -plain of nearest neighbour rods as a function of  $\kappa$ . A pictorial representation of the overlap region between two  $x$ -nearest-neighbour rods of angles  $\theta$  and  $\theta'$  is shown in Fig. 3f. (Overlap regions for neighbours along the  $y$ -direction is related by symmetry.) The equation for the boundary of the overlap region is obtained from simple geometry. For  $\kappa$  near one, the difference of the overlap area from its value at  $\kappa = 1$  vanishes as  $\varepsilon = |\kappa - 1|$  tends to zero, but only as  $\varepsilon \log \varepsilon$ . This logarithmic dependence leads to the logarithmic divergence of  $\partial_\kappa \chi_2$  in Fig. 3e.

The geometrical mechanism behind the phase transition was first reported [29] in one-dimension using a transfer-matrix method. (For a similar origin of singularities in pair-correlation function of 2-d disks see [30].) An exact solution in higher dimensions has been possible only for a small range of  $\kappa$  [25]. Nevertheless, the geometrical transition at  $\kappa = 1$  can be established from its characteristics, notably the logarithmic divergence. Moreover, unlike in a conventional phase transition, non-

analyticities appear even for small systems. Indeed, we observe a negligible system size dependence around the singularity at  $\kappa = 1$  in Fig. 3c. Another signature is that the critical value of  $\kappa$  does not depend on  $\beta$  as long as it remains non-zero.

There are additional geometrical transitions from the overlap between second-nearest-neighbour rods, third-nearest-neighbour rods, and so on. In fact, the overlap function for any pair of rods depends only on the distance between the two centres, and is exactly the same as in the model in one dimension studied earlier [29], which also shows a logarithmic singularity at  $\kappa = 1$ . The overlap function for nearest neighbours undergoes additional singular changes at  $\kappa = 1/2$  (onset of overlap interactions) and  $\kappa = 1/\sqrt{2}$  (see [29] for details), which reflect in  $P(\theta)$  in Fig. 2a. Therefore, including larger neighborhood interactions on the square lattice, where sites are indexed by pairs of integers  $(m, n)$ , geometrical transitions happen at every  $\kappa = z\sqrt{m^2 + n^2}$ , for  $z = \{1/2, 1/\sqrt{2}, 1\}$ . (While  $z = 1$  is redundant, it is kept to emphasize the relation of  $z$  to the different origins of the geometrical singularities in the overlap function when the rod length is half,  $1/\sqrt{2}$ , or equal to the distance between the rod-centres.)

*Phase diagram* — Tracing the phase boundaries of geometrical and symmetry-breaking transitions in the  $(\beta, \kappa)$  plane gives a rich phase diagram shown in Fig. 3g. Unlike the geometrical transitions, the critical  $\kappa$  for the disorder-order transitions depends on  $\beta$ . The infinite  $\beta$  limit corresponds to hard-rod interactions where no overlap is allowed. In this limit the first disorder-order transition is at  $\kappa_c \simeq 0.983$ , and in this case the transition is entropy driven similar to the symmetry breaking transition in hard-spheres [31–33].

Establishing the phase diagram analytically, even for the simplest case where only nearest neighbours interact ( $U_i = 0$  for  $i > 1$ ), requires solving for the largest eigenvalue of a multi-variable transfer operator analogous to the column transfer matrix for the two-dimensional Ising model [34]. An instructive, more tractable case is the Bethe lattice which we discuss below.

*Bethe lattice* — As an analogue of the square lattice we consider a four-coordinated Bethe lattice shown in Fig. 1b, where only rods linked by a single lattice edge interact, i.e.  $U_i = 0$  for  $i > 1$ . Since overlaps depend on the spatial orientation of the rods, we assign to each lattice edge a label x or y depending on the edge orientation in the plane. By construction, the overlap interaction between nearest neighbour rods is the same as on the square lattice.

A Bethe lattice is a tree, thus devoid of loops. It is therefore possible to write a recursion relation for branches at different depths, which led to exact solutions of well-known models [1, 35, 36]. Adapting this idea for our model on the Bethe lattice, we obtain [37] the probability distribution in the thermodynamic limit,

$$P(\theta) = \frac{1}{Z} [g_x^*(\theta)g_y^*(\theta)]^2, \quad (2)$$

where  $Z$  is the normalization, and  $(g_x^*, g_y^*)$  is the stable fixed point solution

$$R_x(g_x^*, g_y^*) = g_x^*, \quad R_y(g_x^*, g_y^*) = g_y^* \quad (3)$$

of the functional flow equations  $R_x(g_x, g_y) \rightarrow g_x$  and  $R_y(g_x, g_y) \rightarrow g_y$  with an initial condition  $g_x(\theta) = g_y(\theta) = 1$  and the generator of the flow

$$R_x(g_x, g_y)[\theta] = \mathcal{N} \cdot \int_0^\pi \frac{d\theta'}{\pi} T_x(\theta, \theta') g_x(\theta') g_y^2(\theta'), \quad (4)$$

( $R_y$  analogously) where the operator  $\mathcal{N} \cdot f(\theta)$  resets the maximum of  $f(\theta)$  to one,  $T_x(\theta, \theta') = e^{-\beta U_1}$  when a pair of  $x$ -neighbour rods of angles  $\{\theta, \theta'\}$  overlap and is equal to one otherwise. The  $T_x$  is constructed from the overlap region in Fig. 3f, and  $T_y$  from the former using symmetry.

For  $\kappa < \frac{1}{2}$ , where rods are not interacting and  $T_x(\theta, \theta') = T_y(\theta, \theta') = 1$ , we see  $g_x^*(\theta) = g_y^*(\theta) = 1$  is a stable fixed point, which gives a uniform distribution  $P(\theta)$  in Eq. (2). For  $\kappa > \frac{1}{2}$ , the fixed point is hard to solve analytically. Nevertheless, a numerical solution is straightforward by implementing the flow equation with a discretised angular range.

Our numerical iteration shows that there is a critical value  $\kappa_c$  that depends on  $\beta$ , below which there is only one stable fixed point. The corresponding  $g_x^*(\theta)$  and  $g_y^*(\theta)$  are not uniform, but they are commensurate with the symmetry around  $\pi/2$ . The  $P(\theta)$  from Eq. (2) shows qualitative agreement with the square-lattice results (compare Fig. 2 with Fig. 4a-b). For  $\kappa > \kappa_c$ , the symmetric fixed point becomes unstable and two new stable fixed points appear which break the symmetry around  $\pi/2$ . The recursion flows into either of the two fixed points with equal probability, corresponding to two equally probable states with broken symmetry, of which one is spontaneously selected in the thermodynamic limit.

The bulk order parameter  $\Psi_2$  involves spatial correlations, which requires the joint probability  $P(\theta, \theta')$ . We chose an analogous quantity  $\hat{\Psi}_2 = |\langle e^{i2\theta} \rangle|$  where  $\langle \cdot \rangle$  denotes averages with  $P(\theta)$ , that captures the continuous disorder-order transition as shown in Fig. 4c (compare with Fig. 3a). Near the transition, the power-law  $\hat{\Psi}_2 \sim (\kappa - \kappa_c)^\beta$  with the critical exponent  $\beta = 1/2$  corresponds to the mean field Ising universality [1].

The geometrical transition is shown in Fig. 4d. Similar to the square lattice, the transition point  $\kappa = 1$  is unaffected by changes in  $\beta$  and the bulk observable  $\langle \chi_2 \rangle$  shows a characteristic logarithmic singularity in its derivative. There are two additional geometrical transitions at  $\kappa = \{1/2, 1/\sqrt{2}\}$ . The relation of these transitions to the singular changes in the overlap region (see e.g. Fig. 3f) can be seen from Eqs. (2)-(4).

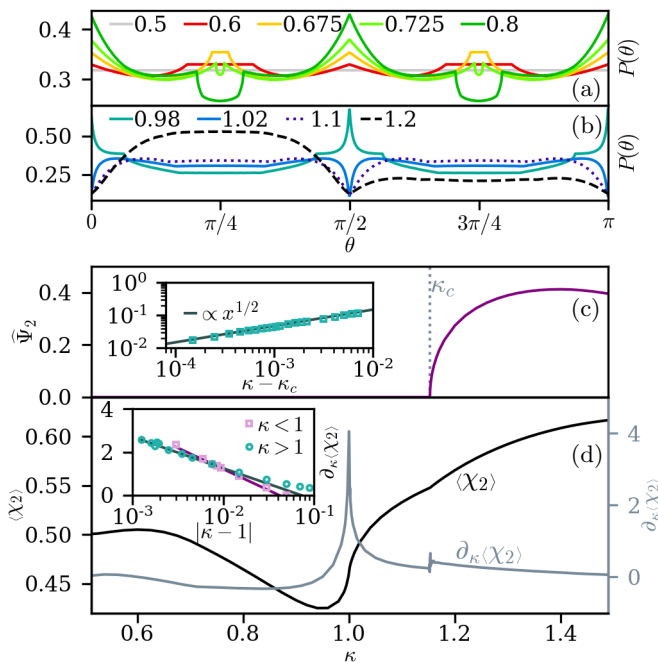


FIG. 4. Bethe lattice – (color online) (a) and (b): Distribution of orientations  $P(\theta)$  at various  $\kappa$  indicated in legend. (a):  $P(\theta)$  is non-uniform for  $\kappa > 1/2$ , with flat parts that vanish at  $\kappa = 1/\sqrt{2}$ , above which  $P(\theta)$  develops two pairs of square-root cusp singularities, that move apart from each other. (b): At  $\kappa = 1$  cusp singularities merge at  $\theta = \{0, \pi/2\}$ , where  $\partial_\kappa P(\theta)$  also changes sign. While  $P(\theta)$  is still symmetric around  $\pi/2$  for  $\kappa = 1.1$  (dotted curve), this symmetry is broken for  $\kappa = 1.2$  (dashed curve). (c): Continuous disorder-order transition at  $\kappa_c \simeq 1.1529$  seen in the order parameter  $\hat{\Psi}_2$ , which vanishes as a power-law (see inset) with decreasing  $\kappa - \kappa_c \geq 0$ . (d): Infinite slope of  $\langle \chi_2 \rangle$  and diverging  $\partial_\kappa \langle \chi_2 \rangle$  at the geometrical transition point  $\kappa = 1$ . The inset shows characteristic logarithmic divergence of  $\partial_\kappa \langle \chi_2 \rangle$  as the transition point is approached. Data for  $\beta U_1 = 1.0$  and an angular discretisation with  $\Delta\theta = \pi/1200$ .

To conclude, several comments are in order. Unlike the square lattice where additional transitions are induced by higher-neighbour overlaps (see Fig. 3g), the Bethe lattice has by construction no additional transitions. However, for the range in  $\kappa$ , where both lattices can be compared, the qualitative behaviour of the orientation distribution  $P(\theta)$  as a function of  $\kappa$  and  $\beta$  is fully captured in this approximation. A similar qualitative phase behaviour with multiple transitions can be seen [37] for the triangular lattice and it is expected to be robust for different shapes of molecules, lattices, and in higher dimensions.

Note that we can think of the full function  $P(\theta)$  as the order parameter, or equivalently an infinity of order parameters, somewhat like the overlap function in the replica theory of spin glasses [38]. The infinity of phases is also reminiscent of ANNNI type models [39].

A comparison of critical exponents shows that on the square lattice the symmetry breaking transitions are

Ising-type. However, they can be different for other lattice geometries, like a triangular lattice. Note that the fixed lattice directions break the continuous symmetry, and the Mermin-Wagner theorem does not apply.

The geometrical transitions are different from the familiar phase transitions in the Ehrenfest classification. Corresponding order parameters change continuously like in a continuous transition, however correlation lengths remain finite [29, 37]. The geometrical transitions are expected to be generic to models where interactions have a non-analytic dependence on control parameters, e.g. an Ising model with an exchange interaction  $J(r)$  that is a non-analytic function of the distance  $r$ .

The question remains to what extent the many transitions seen in our model realize in natural examples. There are known examples of multiple ordered states in organic materials, e.g. Methane absorbed graphite is a two-dimensional example that undergoes an orientational ordering transition [3]. In three dimensions, plastic crystals like Neopentylglycol [19] order in their molecular orientation by cooling below a certain temperature or from lattice contraction by hydrostatic pressure. These changes in orientational order are seen in diffraction experiments [40, 41]. It would be interesting to see if the model discussed in this *Letter*, possibly with additional non-hard-core couplings, can be used to make quantitative agreement with the transitions in experimental systems. The large caloric effect of ordering transitions in plastic crystals makes these questions practically relevant [19, 20].

We thank Sushant Saryal for stimulating discussions. The work of DD is supported by a Senior Scientist Fellowship from the National Academy of Sciences of India. TS acknowledges support of the Department of Atomic Energy, Government of India, under Project Identification No. RTI-4002. TS acknowledges hospitality of the Gulliver Laboratory at ESPCI Paris | PSL, where part of the work was completed.

- 
- [1] R. Baxter, *Exactly Solved Models in Statistical Mechanics*, Dover books on physics (Dover Publications, 2007).
  - [2] S. Friedli and Y. Velenik, *Statistical Mechanics of Lattice Systems: A Concrete Mathematical Introduction* (Cambridge University Press, 2017).
  - [3] D. A. Huckaby, A. M. Dougherty, and A. Pękaliski, Phase transitions in lattice gases of orientable molecules, *Phys. Rev. A* **26**, 3528 (1982).
  - [4] L. Staveley, Thermodynamic studies of molecular rotation in solids, *Journal of Physics and Chemistry of Solids* **18**, 46 (1961).
  - [5] D. B. Abraham and O. J. Heilmann, Lattice models for hydrogen-bonded solvents, *Journal of Statistical Physics* **4**, 15 (1972).
  - [6] O. J. Heilmann and D. A. Huckaby, Phase transitions in lattice gas models for water, *Journal of Statistical Physics*

- 20**, 371 (1979).
- [7] B. W. Southern and D. A. Lavis, A model for adsorbed monolayers of orientable molecules, *Journal of Physics C: Solid State Physics* **12**, 5333 (1979).
- [8] L. Onsager, The effects of shape on the interaction of colloidal particles, *Ann. N. Y. Acad. Sci.* **51**, 627 (1949).
- [9] J. L. Lebowitz and G. Gallavotti, Phase transitions in binary lattice gases, *Journal of Mathematical Physics* **12**, 1129 (1971).
- [10] Y. Kantor and M. Kardar, One dimensional gas of hard needles model for correlated molecular rotation, *Phys. Rev. E* **79**, 041109 (2009).
- [11] P. Gurin and S. Varga, Towards understanding the ordering behavior of hard needles: Analytical solutions in one dimension, *Phys. Rev. E* **83**, 061710 (2011).
- [12] P. J. Flory and G. Gee, Statistical thermodynamics of semi-flexible chain molecules, *Proceedings of the Royal Society of London. Series A. Mathematical and Physical Sciences* **234**, 60 (1956).
- [13] G. I. Ågren and D. E. Martire, End-chain flexibility and the nematic-isotropic transition in liquid crystals: A lattice model of hard particles with rigid, rodlike, central cores and semiflexible pendant segments, *The Journal of Chemical Physics* **61**, 3959 (1974).
- [14] O. J. Heilmann and E. Praestgaard, Crystalline ordering in lattice models of hard rods with nearest neighbour attraction, *Chemical Physics* **24**, 119 (1977).
- [15] A. Ghosh and D. Dhar, On the orientational ordering of long rods on a lattice, *Europhysics Letters (EPL)* **78**, 20003 (2007).
- [16] J. Timmermans, Plastic crystals: A historical review, *Journal of Physics and Chemistry of Solids* **18**, 1 (1961).
- [17] J. C. W. Folmer, R. L. Withers, T. R. Welberry, and J. D. Martin, Coupled orientational and displacive degrees of freedom in the high-temperature plastic phase of the carbon tetrabromide  $\alpha$ -CBr<sub>4</sub>, *Phys. Rev. B* **77**, 144205 (2008).
- [18] L. C. Towle, The plastic properties of carbon tetrabromide, *Applied physics* **2**, 187 (1973).
- [19] B. Li, Y. Kawakita, S. Ohira-Kawamura, T. Sugahara, H. Wang, J. Wang, Y. Chen, S. I. Kawaguchi, S. Kawaguchi, K. Ohara, K. Li, D. Yu, R. Mole, T. Hattori, T. Kikuchi, S.-i. Yano, Z. Zhang, Z. Zhang, W. Ren, S. Lin, O. Sakata, K. Nakajima, and Z. Zhang, Colossal barocaloric effects in plastic crystals, *Nature* **567**, 506 (2019).
- [20] D. Chandra, W. Ding, R. A. Lynch, and J. J. Tomlinson, Phase transitions in “plastic crystals”, *Journal of the Less Common Metals* **168**, 159 (1991).
- [21] G. Guthrie and J. McCullough, Some observations on phase transformations in molecular crystals, *Journal of Physics and Chemistry of Solids* **18**, 53 (1961).
- [22] S. Yashonath and C. Rao, Monte carlo simulation of the crystal to plastic crystal transition in carbon tetrachloride, *Chemical Physics Letters* **119**, 22 (1985).
- [23] L. M. Casey and L. K. Runnels, Model for correlated molecular rotation, *J. Chem. Phys.* **51**, 5070 (1969).
- [24] B. C. Freasier and L. K. Runnels, Classical rotators on a linear lattice, *The Journal of Chemical Physics* **58**, 2963 (1973).
- [25] S. Saryal and D. Dhar, Exact results for interacting hard rigid rotors on a d-dimensional lattice (2022), arXiv:2201.12866 [cond-mat.stat-mech].
- [26] P. de Gennes and J. Prost, *The Physics of Liquid Crystals*, International Series of Monographs on Physics (Clarendon Press, 1993).
- [27] P. J. Steinhardt, D. R. Nelson, and M. Ronchetti, Bond-orientational order in liquids and glasses, *Phys. Rev. B* **28**, 784 (1983).
- [28] W. Mickel, S. C. Kapfer, G. E. Schröder-Turk, and K. Mecke, Shortcomings of the bond orientational order parameters for the analysis of disordered particulate matter, *The Journal of Chemical Physics* **138**, 044501 (2013).
- [29] S. Saryal, J. U. Klamser, T. Sadhu, and D. Dhar, Multiple singularities of the equilibrium free energy in a one-dimensional model of soft rods, *Phys. Rev. Lett.* **121**, 240601 (2018).
- [30] F. H. Stillinger, Pair distribution in the classical rigid disk and sphere systems, *Journal of Computational Physics* **7**, 367 (1971).
- [31] S. Asakura and F. Oosawa, On interaction between two bodies immersed in a solution of macromolecules, *The Journal of Chemical Physics* **22**, 1255 (1954).
- [32] J. F. Joanny, L. Leibler, and P. G. De Gennes, Effects of polymer solutions on colloid stability, *Journal of Polymer Science: Polymer Physics Edition* **17**, 1073 (1979).
- [33] W. Krauth, *Statistical Mechanics: Algorithms and Computations*, Oxford Master Series in Physics (OUP Oxford, 2006).
- [34] T. D. Schultz, D. C. Mattis, and E. H. Lieb, Two-dimensional ising model as a soluble problem of many fermions, *Rev. Mod. Phys.* **36**, 856 (1964).
- [35] D. Dhar and S. N. Majumdar, Abelian sandpile model on the bethe lattice, *Journal of Physics A: Mathematical and General* **23**, 4333 (1990).
- [36] F. Peruggi, F. di Libertò, and G. Monroy, The potts model on bethe lattices. i. general results, *Journal of Physics A: Mathematical and General* **16**, 811 (1983).
- [37] J. Klamser, T. Sadhu, and D. Dhar, In preparation, (2022).
- [38] M. Mezard, G. Parisi, and M. Virasoro, *Spin Glass Theory and Beyond* (WORLD SCIENTIFIC, 1986).
- [39] W. Selke, The anmi model — theoretical analysis and experimental application, *Physics Reports* **170**, 213 (1988).
- [40] L. Temleitner and L. Pusztai, The origin of diffuse scattering in crystalline carbon tetraiodide, *Journal of Physics: Condensed Matter* **25**, 454209 (2013).
- [41] M. More, J. Lefebvre, B. Hennion, B. M. Powell, and C. M. E. Zeyen, Neutron diffuse scattering in the disordered phase of CrBr<sub>4</sub>. i. experimental. elastic and quasi-elastic coherent scattering in single crystals, *Journal of Physics C: Solid State Physics* **13**, 2833 (1980).